Biochemical and Biophysical Research Communications 380 (2009) 183–187

Contents lists available at ScienceDirect

Biochemical and Biophysical Research Communications

journal homepage: www.elsevier.com/locate/ybbrc

# Contribution of globular death domains and unstructured linkers to MyD88·IRAK-4 heterodimer formation: An explanation for the antagonistic activity of MyD88s

Elena Mendoza-Barberá [a,b,1], María Ángeles Corral-Rodríguez [a,1], Alessandra Soares-Schanoski [b], Milko Velarde [c], Sofia Macieira [c], Albrecht Messerschmidt [c], Eduardo López-Collazo [b], Pablo Fuentes-Prior [a,*]

[a] Cardiovascular Research Center and Institut de Recerca, Hospital de la Santa Creu i Sant Pau, Sant Antoni Maria Claret 167, 08025 Barcelona, Spain
[b] Laboratory of Tumor Immunology, Research Unit, 'La Paz' Hospital, 28046 Madrid, Spain
[c] Proteomics and Signal Transduction, Max-Planck-Institut für Biochemie, 82152 Munich, Germany

ARTICLE INFO

*Article history:*
Received 29 December 2008
Available online 22 January 2009

*Keywords:*
MyD88
IRAK
Death domain
Toll-like receptor
Monocytes/macrophages

ABSTRACT

Homotypic interactions of death domains (DD) mediate complex formation between MyD88 and IL-1 receptor-associated kinases (IRAKs). A truncated splice variant of MyD88, MyD88s, cannot recruit IRAK-4 and fails to elicit inflammatory responses. We have generated recombinant DD of MyD88 and IRAK-4, both alone and extended by the linkers to TIR or kinase domains. We show that both MyD88 DD variants bind to the linker-extended IRAK-4 DD and pull-down full-length IRAK-4 from monocyte extracts. By contrast, residues up to $Glu^{116}$ from the DD–kinase connector of IRAK-4 are needed for strong interactions with the adaptor. Our findings indicate that residues 110–120, which form a C-terminal extra helix in MyD88, but not the irregular linker between DD and TIR domains, are required for IRAK-4 recruitment, and provide a straightforward explanation for the negative regulation of innate immune responses mediated by MyD88s.



Engagement of Toll-like receptors (TLRs) and IL-1 receptor (IL-1R) enforces multimerization [1] and recruitment of adaptors such as MyD88 through homotypic interactions of their cytosolic TIR domains [2,3], which in turn recruits IRAK-1 and 4 (reviewed in [4]). Formation of MyD88·IRAK-1·IRAK-4 multimers triggers a cascade of (auto)phosphorylation reactions that culminates in activation of NF-κB/AP-1, and transcription of multiple genes that regulate inflammatory responses [5]. MyD88–IRAK complex formation relies on homotypic interactions of death domains (DD), which belong to a large superfamily of α-helical modules [6].

The crystal structure between DDs of the *Drosophila* kinase Pelle and its adaptor Tube [7], which function downstream of Toll engagement in insects, provided first structural information about homotypic DD-mediated complex formation. However, although the Toll → MyD88 → Tube → Pelle cascade is functionally equivalent to that of TLR → MyD88 → IRAK-4 → IRAK-1 (Fig. 1A and Refs. [8,9]), there are major differences between mammalian and insect immune responses. Most relevant, mammals lack a Tube ortholog, whose role appears to be assumed by IRAK-4 [9–14]. A recent study confirmed that IRAK-4 is part of a stable complex with IL-1R and MyD88 formed upon IL-1 stimulation [15].

The truncated splice variant p.Glu110_Leu154del MyD88, termed MyD88 short (MyD88s), is overexpressed in monocytes upon continuous stimulation with LPS or proinflammatory cytokines [16,17]. MyD88s is unable to recruit IRAK-4, and accordingly downregulates inflammatory responses to multiple stimuli [11] (see Fig. 1B for the schematic domain organization of MyD88 and IRAK-4). It has been proposed that these findings imply a critical role for the DD–TIR linker of the adaptor in kinase recruitment.

Here, we have used recombinant truncated variants of MyD88 and IRAK-4 to show that IRAK-4 recruitment to IL-1R·MyD88/TLR·MyD88 complexes requires interactions mediated by the C-terminal helix from the adaptor DD and the DD–kinase linker of IRAK-4, similar to those observed in Tube·Pelle.

## Materials and methods

*Materials.* B-PER® was from Pierce, Glu-C and chymotrypsin from Roche Diagnostics, Ni–NTA–agarose matrix from QIAGEN, PVDF membranes and centrifugal filter devices from Millipore,

*Abbreviations:* DD, death domain; IRAK, IL-1 receptor-associated kinase; TLR, Toll-like receptor; TIR, Toll–IL-1 receptor.

* Corresponding author. Fax: +34 93 556 5559.
*E-mail addresses:* pfuentes@csic-iccc.org, pfuentes@santpau.cat (P. Fuentes-Prior).

[1] These authors contributed equally to this study.

0006-291X/$ - see front matter © 2009 Elsevier Inc. All rights reserved.
doi:10.1016/j.bbrc.2009.01.069

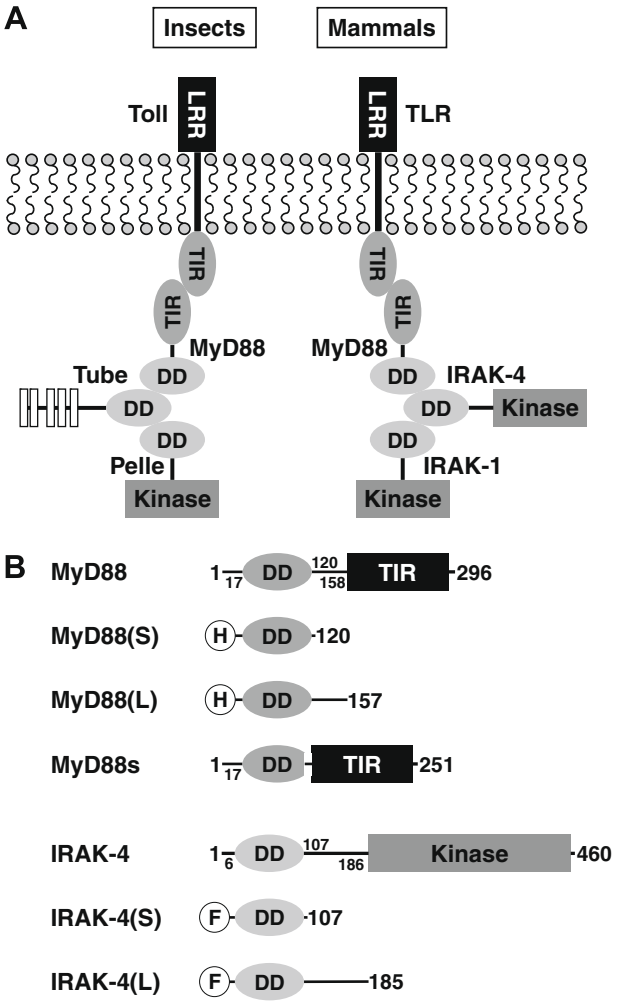


**Fig. 1.** Comparison of Toll/TLR-mediated innate immune responses in insects and mammals. (A) Schematic representation of complex formation downstream of Toll (insects, left panel) and TLR (mammals, right panel). Notice that insects possess a second non-enzymatic adaptor, Tube; IRAK-4 appears to assume this scaffolding role in the mammalian system. (B) Domain organization of human MyD88 and IRAK-4. Numbers indicate approximate domain boundaries (see also Supplementary Fig. 1). The structure of truncated variants generated in the current study is also given; encircled letters H and F represent tags attached to these recombinant forms (6× His and FLAG, respectively). Notice that the natural truncated variant, MyD88s, lacks the last helix of the death domain from the adaptor along with most of the DD–TIR linker.

and autoradiography films from Agfa-Gevaert. Molecular weight markers were purchased from Invitrogen. The detergent screen kit was from Hampton Research. All other chemicals, of the highest purity grade available, were purchased from Sigma–Aldrich or Merck.

*Bioinformatics analysis and modeling.* Sequences were aligned using ClustalW (http://www.ebi.ac.uk/clustalw/) and the preliminary alignment manually corrected based on available structural information [7,18], secondary structure predictions (http://cubic.bioc.columbia.edu/predictprotein/), and order/disorder propensities. Homology modeling was performed using SWISS-MODEL (http://swissmodel.expasy.org//SWISS-MODEL.html) and the structures of murine IRAK-4 (PDB: 2A9I) or Pelle DDs (1D2Z_C). Protein–protein interaction surfaces were predicted with the PPI server (http://www.bioinformatics.leeds.ac.uk/ppi_pred). Structure figures were generated with PyMOL (http://www.pymol.org).

*Cloning and mutagenesis.* The limits of truncated MyD88 and IRAK-4 forms used in the current work are indicated in Fig. 1B and Supplementary Table 1. All fragments were designed as optimized synthetic genes, generated by oligonucleotide assembly, and cloned into plasmid pET-3a at Entelechon. An IRAK-4(L) variant truncated at $Lys^{125}$ was generated with the QuickChange® Site-Directed Mutagenesis Kit (Strategene) and primers IRAK-4_K125stop_fwd (5′-CGAACACTCTGCCGTCT**TAA**GAGGCGATTACTG TG-3′) and IRAK-4_K125stop_rev (5′-CACAGTAATCGCCTC**TTA**AGA CGGCAGAGTGTTCG-3′). (The introduced stop codon is in bold).

*Protein expression, renaturation, and purification. Escherichia coli* BL21(DE3) or derivatives thereof were grown in LB medium containing appropriate antibiotics following standard protocols. Cells were disrupted with B-PER (100 μl/ml culture), supplemented with 10 mM $MgCl_2$, 20 mM 2-mercaptoethanol (2-ME), and 1 U/ml DNase I. After centrifugation at 10,000*g* the pellet was washed with the same volume of B-PER solution containing 200 mM NaCl, 20 mM 2-ME, 1 mM EDTA, and 10 mM imidazole, resuspended in wash/binding buffer (25 mM sodium phosphate, pH 7.8, 300 mM NaCl, 10 mM 2-ME, 500 μM EDTA, 0.5% (w/v) β-octylglucoside), and insoluble proteins extracted with urea.

MyD88(L) was recovered from the soluble fraction of BL21(DE3)pLysS cells, and was purified using Ni–NTA–agarose matrix. Other recombinant proteins as well as mixtures of urea-denatured MyD88 and IRAK-4 variants were refolded at 4 °C essentially following the fractional factorial protein-folding screen [19]. After centrifugation, protein solutions were buffer-exchanged and purified by metal affinity chromatography (MyD88 variants and their complexes) or by ion-exchange chromatography on Q-Sepharose (IRAK-4 variants). Protein concentrations were determined either with the BCA protein assay kit (Pierce) or from the absorbance at 280 nm using absorption coefficients given in Supplementary Table 1.

*Monocyte isolation and culture.* PBMC were isolated and cultured to a density of $10^6$ cells/ml as previously reported [20]. The supernatant was then removed and adherent cells ($2 \times 10^6$ per well) were cultured in the same medium supplemented with 10% heat-inactivated fetal bovine serum. Monocytes were lysed at 4 °C using ice-cold Cell Lysis Buffer (10 mM imidazole, pH 7.3, 500 mM NaCl, 0.5% Triton X-100, 0.2 mM sodium orthovanadate, 0.2 mM PMSF, and 2 mM $NaN_3$). Cellular debris was removed by centrifugation at 15,000*g*, and the supernatant was aliquoted and stored at −20 °C until further use.

*SDS–PAGE and Western blotting.* Proteins were separated on SDS–Tris–Tricine polyacrylamide gels using a Bio-Rad apparatus. Gels were either stained with Coomassie Brilliant Blue or silver, or transferred to PVDF membranes using a fully submerged transfer cell (Bio-Rad). For immunoblotting, membranes were blocked in TBS containing 5% skim milk, incubated for 1 h at room temperature with the primary antibody, and thoroughly washed with TBS; membranes were similarly treated with the secondary antibody. The following antibodies were used at indicated dilutions: mouse anti-His monoclonal antibody (Amersham Biosciences; 1:3000), mouse anti-FLAG® M2 (Sigma–Aldrich; 1:3000), goat anti-human IRAK-4 polyclonal antibody (R&D Systems; 1 μg/ml), goat anti-mouse IgG horseradish peroxidase conjugate (Pierce; 1:5000), and donkey anti-goat conjugate (R&D Systems; 1:1000). Blots were revealed with SuperSignal chemoluminescence system (Pierce) according to the manufacturer's instructions and exposed to autoradiography films.

*Limited proteolysis.* Protein samples were incubated at 25 °C with Glu-C or chymotrypsin (enzyme:protein ratio, 1:100). Aliquots were taken at various times, and reactions stopped by adding Laemmli sample buffer and incubating at 95 °C for 5 min.

*Binding assays in solution.* Purified recombinant proteins were mixed at 37 °C, and then incubated for 15 min with excess Ni–NTA–agarose matrix. After centrifugation at 800×*g*, the matrix was thoroughly washed with binding buffer containing 10 mM

imidazole. Specifically bound proteins were finally eluted with binding buffer supplemented with up to 500 mM imidazole. Alternatively, purified MyD88(S) or MyD88(L) were incubated with cytosolic extracts from human monocytes, and treated as above. Pulled-down monocyte proteins were detected with an anti-human IRAK-4 polyclonal antibody.

## Results and discussion

### *Expression of death domains from MyD88 and IRAK-4*

Inspection of a structure-based sequence alignment of MyD88 and IRAK-4 DDs indicates that residues $Ile^{109}$ to $Lys^{119}$ in mammalian MyD88 are highly similar to those of *Drosophila* Pelle (Supplementary Fig. 1). This observation and the results of secondary structure predictions allow us to predict with high confidence that MyD88 possesses a seventh, C-terminal helix, in addition to the conserved framework of six antiparallel helices observed in Tube [7], as well as in IRAK-4 [18], and in other DD superfamily members from e.g. caspases and their adaptors.

To analyze the contributions of globular/unstructured regions of human MyD88 and IRAK-4 to complex formation, we cloned, overexpressed and purified to homogeneity "short" and "long" variants of their DDs (Fig. 1B). Purity and authenticity of recombinant proteins were assessed by SDS–PAGE (Supplementary Fig. 2A), Western blotting with appropriate anti-tag monoclonal antibodies (Supplementary Fig. 2B and C) and MALDI-TOF analysis of tryptic digests.

Dynamic light scattering analysis revealed that these recombinant MyD88 and IRAK-4 variants form large aggregates in solution (not shown). However, several independent observations strongly suggest that these aggregates contain properly folded DDs. (1) Most of the sixteen refolding conditions routinely tested were successful with all recombinant proteins. (2) Glu-Xxx scissile peptide bonds within the irregular C-terminal tails but not the globular death domains in MyD88(L) and IRAK-4(L) are susceptible to Glu-C cleavage (Supplementary Fig. 3). According to the distances migrated by digestion products in SDS–PAGE, the C-terminal residues of stable fragments are $Glu^{143}$ (MyD88) and $Glu^{116}$ in IRAK-4. Finally, (3) IRAK-4(S) crystallizes under conditions similar to those reported for its murine counterpart [18].

This strong tendency to self-aggregation is consistent with observations of large discrete cytosolic aggregates formed by full-length MyD88 overexpressed in diverse cell lines [21–24]; a recent work demonstrates that the entire non-TIR region is responsible for this pronounced cytosolic aggregation [25]. Our findings are reminiscent of *in vivo* TLR oligomerization to form large "receptosomes", which in turn recruit MyD88 [1].

### *Isolated DDs of MyD88 and IRAK-4 form a stable complex in solution*

It has not been unambiguously established whether additional cofactors are necessary for MyD88-mediated IRAK recruitment *in vivo*. In initial assays we observed only partial complex formation (Supplementary Fig. 4), apparently because aggregation of individual DDs interferes with heterodimer formation *in vitro*. However, using low protein concentrations and specific non-ionic detergents (Supplementary Fig. 5) allowed quantitative formation of the MyD88(L)·IRAK-4(L) complex in solution, as demonstrated by pull-down of increasing amounts of IRAK-4(L) by the Ni–NTA matrix (Fig. 2A). Interestingly, at low IRAK-4 concentrations no heterocomplex was detected, and the MyD88(L) linker was partially cleaved by a contaminating protease. Degradation was prevented at higher IRAK-4(L) concentrations that support complex formation, suggesting protection of the linkers in the heterodimer.

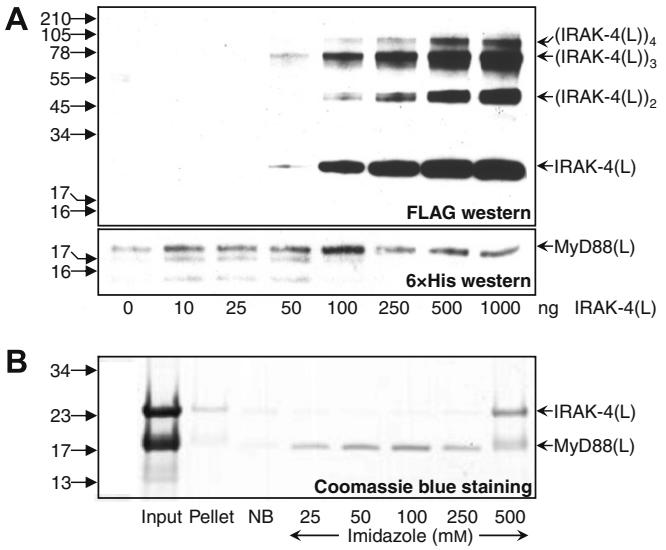


**Fig. 2.** Formation of a stable MyD88(L)·IRAK-4(L) heterodimer in solution. (A) Various amounts of IRAK-4(L) were incubated with 1 μg purified MyD88(L) for 2 h at 37 °C. Next, equal volumes of Ni–NTA matrix were added to these mixtures. After centrifugation, the affinity matrix was thoroughly washed with 10 mM imidazole before eluting specifically bound proteins with Laemmli sample buffer. Protein fractions were analyzed by Western blot using anti-FLAG (upper panel) or anti-6× His (lower panel) antibodies. (B) A mixture of urea-denatured IRAK-4(L) and MyD88(L) (input) was refolded by rapid dilution. After centrifugation to remove insoluble material (pellet), proteins that specifically bind Ni–NTA–agarose were eluted with increasing imidazole concentrations.

To confirm complex formation while minimizing interference of aggregation, we refolded mixtures of urea-denatured MyD88(L) and IRAK-4(L) by rapid dilution. We could identify several conditions in which the soluble MyD88(L)·IRAK-4(L) complex was quantitatively recovered by metal affinity chromatography. Based on the condition that gave best results, we established a larger-scale refolding procedure in which a protein mixture containing a slight molar excess of MyD88(L) is incubated O.N. in 50 mM sodium phosphate, pH 7.0, 264 mM NaCl, 11 mM KCl, 2.2 mM $MgCl_2$, 2.2 mM $CaCl_2$, 440 mM sucrose, 1 mM GSH, and 0.1 mM GSSG. This co-renaturation procedure allows reproducible generation of the MyD88(L)·IRAK-4(L) heterodimer (Fig. 2B), providing a simple means for analysis of DD-mediated complex formation. Notably, the MyD88(L)·IRAK-4(L) complex bound more tightly to the metal affinity matrix than the free adaptor DD, pointing to formation of dimers or higher order aggregates of the heterodimer. In this regard, MyD88 is known to dimerize following receptor recruitment *in vivo* [26], and recent evidence indicates that enforced adaptor dimerization suffices to trigger signaling [27]. We conclude that the C-terminal TIR (MyD88) and kinase modules (IRAK-4) are dispensable for kinase recruitment.

### *The DD-TIR linker of MyD88 is not required for IRAK-4 recruitment*

To determine whether the interdomain connectors of MyD88 and IRAK-4 are required for complex formation, we performed experiments essentially as described above, but replacing the "long" forms of the recombinant proteins by their linker-less counterparts. First, we demonstrated that MyD88(S) forms a stable complex with IRAK-4(L) (Supplementary Fig. 6A). To verify the ability of isolated MyD88 DD to bind full-length IRAK-4 we incubated purified MyD88(L) or MyD88(S) with increasing amounts of human monocyte extracts. After addition of Ni–NTA matrix, specifically bound proteins were identified *via* immunoblotting with an anti-human IRAK-4 polyclonal antibody. The results of this

experiment demonstrate quantitative, saturable binding of natural IRAK-4 by both truncated forms of MyD88 (Fig. 3), corroborating that the DD–TIR linker of the adaptor (residues 121–158) is not required for kinase binding.

Previous results with the truncated variant MyD88s had indicated that adaptor residues 110–154 are strictly required for IRAK-4 recruitment *in vivo* [11,17]. This apparent contradiction strongly suggests that MyD88 residues $Glu^{110}$ to $Gln^{120}$ (DD helix α7) play a major functional role in this regard. In support of this hypothesis, mutation p.Tyr116Cys in murine MyD88 results in reduced immune responses to several pathogen-associated ligands [28].

### *Residues up to $Glu^{116}$ from the DD–kinase linker of IRAK-4 are required for MyD88 binding*

We next analyzed whether the IRAK-4 linker was required for complex formation with the adaptor. IRAK-4(S) bound only weakly to the DD-only form of MyD88 (compare intensity of bands in the anti-FLAG Western blots; Supplementary Fig. 6A and B), and similar results were obtained with MyD88(L) (not shown). These findings indicate that the DD–kinase connector of IRAK-4 is important for heterodimer formation. To define the linker region needed for complexation, we compared accessibility of this polypeptide stretch to proteolytic attack in the presence and absence of MyD88(S). Similar to the experiments performed for protein characterization (Supplementary Fig. 3), we incubated the MyD88(S)·IRAK-4(L) complex with Glu-C for various times. Presence of the adaptor completely abolished proteolysis of the $Glu^{116}$–$Ala^{117}$ peptide bond, while the $Glu^{143}$–$Leu^{144}$ site was hydrolyzed as in free IRAK-4(L), albeit with slower kinetics (Supplementary Fig. 7A, upper panel). By contrast, chymotrypsinolysis of free and adaptor-bound IRAK-4(L) was essentially identical (Supplementary Fig. 8), indicating that the $Phe^{127}$–$Glu^{128}$ site is not protected in the MyD88·IRAK-4 complex. Finally, we verified normal complex formation with an IRAK-4 variant truncated after $Lys^{125}$ (Supplementary Fig. 7B).

In conclusion, DD–kinase linker residues in IRAK-4 up to at least $Glu^{116}$, but not beyond $Lys^{125}$, are critical for recruitment by MyD88. Additional support for our hypothesis comes from the observation that an extended polypeptide stretch from Tube located downstream of the globular death domain is "clamped" between helix α7 and the main globular DD of Pelle [7].

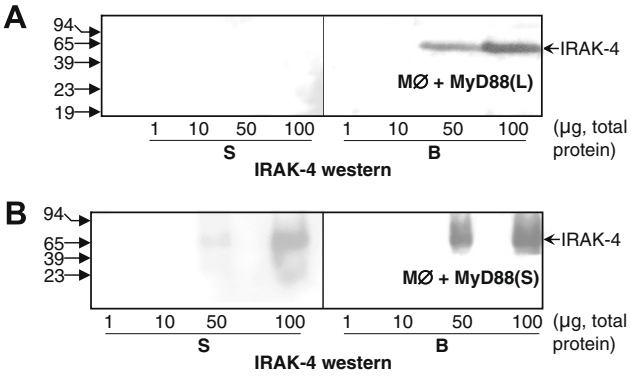


**Fig. 3.** MyD88 DD pulls down natural IRAK-4 from monocyte extracts. Fixed amounts (2 µg) of MyD88(L) (A) or MyD88(S) (B) were added to increasing quantities of cytosolic extracts from human monocytes. After incubation with Ni–NTA–agarose and centrifugation, the supernatants (S) were precipitated with five volumes of cold acetone, while specifically bound proteins (B) were recovered with Laemmli buffer after thoroughly washing the affinity matrix. Samples were analyzed by Western blotting with an anti-IRAK-4 antibody.

### *A model of MyD88·IRAK-4 heterodimer*

To rationalize on a structural basis the topological equivalence of MyD88–Pelle and IRAK-4–Tube pairs suggested by the results discussed above, we generated 3D models for DDs of human MyD88 and IRAK-4 (Fig. 4A and B). Although residues involved in intermolecular contacts in the Pelle·Tube heterodimer are generally not conserved in mammalian MyD88/IRAK-4 (Supplementary Figs. 1 and 3B), a model of their putative complex could be constructed by combining features of equivalent Pelle–Tube [7] and RAIDD–PIDD type II DD interfaces [29] (Fig. 4C). This model is also supported by predictions of surface areas of MyD88 and IRAK-4 DDs that are important for protein–protein interactions (Supplementary Tables 2 and 3). Along these lines, it is noteworthy that the Pelle–Tube interface shows considerable plasticity, as revealed by significant differences between the two independent complex molecules found in the asymmetric unit.

In support of our model, we notice that adaptor dimerization would not interfere with IRAK-4 recruitment, in line with experimental observations. Furthermore, the relative location of binding sites suggests that MyD88 would not directly interact with IRAK-1, similar to what has been demonstrated for the *Drosophila*

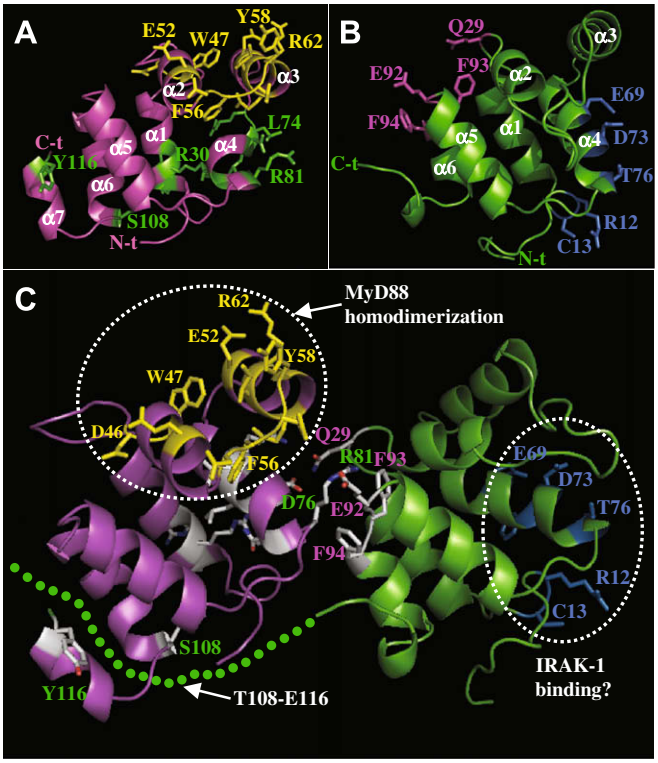


**Fig. 4.** Model of DD-mediated IRAK recruitment to MyD88. (A and B) 3D models of DDs from human MyD88 and IRAK-4. α-Helices and the N- and C-termini are marked. Selected residues within the two highest scoring patches identified by PPI-Pred are indicated with their side chain atoms, colored and labeled yellow and green (MyD88) or blue and pink (IRAK-4), respectively. The highest scoring patch in MyD88 is a cluster of polar/aromatic residues from helices α2/α3 and their connecting loop; it appears to represent the MyD88–MyD88 interaction area, as replacement of $Phe^{56}$ by an asparagine impairs DD-mediated dimerization of the adaptor [26]. The second highest-scoring patch is predicted to be the IRAK-4 binding surface. For IRAK-4 DD, the predicted MyD88-interactive region was also identified as the second highest-scoring area. The most likely protein–protein interaction site for this domain involves a distinct cluster of N-terminal and adjacent residues from helices α1 and α4. This patch, topologically equivalent to the IRAK-4 binding site on MyD88, might represent the IRAK-1 – interaction region. (C) Docking model of the putative MyD88·IRAK-4 heterodimer. (For interpretation of the references to colour in this figure legend, the reader is referred to the web version of this article.)

MyD88·Tube·Pelle heterotrimer [9,30]. Structural and functional investigations now in progress should refine this model and identify residues critical for formation of the MyD88·IRAK-4·IRAK-1 complex.

## Acknowledgments

This work was supported by grants SAF2004-00543, SAF2007-64140 (P.F.-P.), and SAF2006-1256 (E.L.-C.) from the Spanish MEC and by Fundación MMA (E.L.-C.). S.M., A.M., and M.V. acknowledge financial support by the European Commission (Contract No. 031220, "Spine2-Complexes"). E.M.-B. acknowledges a scholarship from Baxter S.L.M.-A.C.R. was supported by FPI Grant BES2005-6841 from Spanish MEC, and A.S.-S. by a CALPES scholarship.

## Appendix A. Supplementary data

Supplementary data associated with this article can be found, in the online version, at doi:10.1016/j.bbrc.2009.01.069.

## References

[1] A. Visintin, E. Latz, B.G. Monks, T. Espevik, D.T. Golenbock, Lysines 128 and 132 enable lipopolysaccharide binding to MD-2, leading to Toll-like receptor-4 aggregation and signal transduction, J. Biol. Chem. 278 (2003) 48313–48320.
[2] S. Akira, K. Takeda, Toll-like receptor signalling. Nat. Rev. Immunol. 4 (2004) 499–511.
[3] H. Wesche, W.J. Henzel, W. Shillinglaw, S. Li, Z. Cao, MyD88: an adapter that recruits IRAK to the IL-1 receptor complex, Immunity 7 (1997) 837–847.
[4] S. Janssens, R. Beyaert, Functional diversity and regulation of different interleukin-1 receptor-associated kinase (IRAK) family members, Mol. Cell 11 (2003) 293–302.
[5] N. Silverman, T. Maniatis, NF-{kappa}B signaling pathways in mammalian and insect innate immunity, Genes Dev. 15 (2001) 2321–2342.
[6] H.H. Park, Y.C. Lo, S.C. Lin, L. Wang, J.K. Yang, H. Wu, The death domain superfamily in intracellular signaling of apoptosis and inflammation, Annu. Rev. Immunol. 25 (2007) 561–586.
[7] T. Xiao, P. Towb, S.A. Wasserman, S.R. Sprang, Three-dimensional structure of a complex between the death domains of Pelle and Tube, Cell 99 (1999) 545–555.
[8] T. Horng, R. Medzhitov, *Drosophila* MyD88 is an adapter in the Toll signaling pathway, Proc. Natl. Acad. Sci. USA 98 (2001) 12654–12658.
[9] H. Sun, B.N. Bristow, G. Qu, S.A. Wasserman, A heterotrimeric death domain complex in Toll signaling, Proc. Natl. Acad. Sci. USA 99 (2002) 12871–12876.
[10] S. Li, A. Strelow, E.J. Fontana, H. Wesche, IRAK-4: a novel member of the IRAK family with the properties of an IRAK-kinase, Proc. Natl. Acad. Sci. USA 99 (2002) 5567–5572.
[11] K. Burns, S. Janssens, B. Brissoni, N. Olivos, R. Beyaert, J. Tschopp, Inhibition of interleukin 1 receptor/Toll-like receptor signaling through the alternatively spliced, short form of MyD88 is due to its failure to recruit IRAK-4, J. Exp. Med. 197 (2003) 263–268.
[12] E. Lye, C. Mirtsos, N. Suzuki, S. Suzuki, W.-C. Yeh, The role of interleukin 1 receptor-associated kinase-4 (IRAK-4) kinase activity in IRAK-4-mediated signaling, J. Biol. Chem. 279 (2004) 40653–40658.
[13] T. Kawagoe, S. Sato, A. Jung, M. Yamamoto, K. Matsui, H. Kato, S. Uematsu, O. Takeuchi, S. Akira, Essential role of IRAK-4 protein and its kinase activity in Toll-like receptor-mediated immune responses but not in TCR signaling, J. Exp. Med. 204 (2007) 1013–1024.
[14] T.W. Kim, K. Staschke, K. Bulek, J. Yao, K. Peters, K.-H. Oh, Y. Vandenburg, H. Xiao, W. Qian, T. Hamilton, B. Min, G. Sen, R. Gilmour, X. Li, A critical role for IRAK4 kinase activity in Toll-like receptor-mediated innate immunity, J. Exp. Med. 204 (2007) 1025–1036.
[15] C. Brikos, R. Wait, S. Begum, L.A.J. O'Neill, J. Saklatvala, Mass spectrometric analysis of the endogenous IL-1RI signalling complex formed after IL-1 binding, identifies IL-1RAcP, MyD88 and IRAK-4 as the stable components, Mol. Cell. Proteomics 6 (2007) 1551–1559.
[16] S. Janssens, K. Burns, E. Vercammen, J. Tschopp, R. Beyaert, MyD88s, a splice variant of MyD88, differentially modulates NF-κB- and AP-1-dependent gene expression, FEBS Lett. 548 (2003) 103–107.
[17] S. Janssens, K. Burns, J. Tschopp, R. Beyaert, Regulation of interleukin-1- and lipopolysaccharide-induced NF-[kappa]B activation by alternative splicing of MyD88, Curr. Biol. 12 (2002) 467–471.
[18] M.V. Lasker, M.M. Gajjar, S.K. Nair, Molecular structure of the IL-1R-associated kinase-4 death domain and its implications for TLR signaling, J. Immunol. 175 (2005) 4175–4179.
[19] N. Armstrong, A. de Lencastre, E. Gouaux, A new protein folding screen: application to the ligand binding domains of a glutamate and kainate receptor and to lysozyme and carbonic anhydrase, Protein Sci. 8 (1999) 1475–1483.
[20] C. del Fresno, K. Otero, L. Gómez-García, M.C. González-León, L. Soler-Ranger, P. Fuentes-Prior, P. Escoll, R. Baos, L. Caveda, F. García, F. Arnalich, E. López-Collazo, Tumor cells deactivate human monocytes by up-regulating IL-1 receptor associated kinase-M expression via CD44 and TLR4, J. Immunol. 174 (2005) 3032–3040.
[21] F. Jaunin, K. Burns, J. Tschopp, T.E. Martin, S. Fakan, Ultrastructural distribution of the death-domain-containing MyD88 protein in HeLa cells, Exp. Cell Res. 243 (1998) 67–75.
[22] T. Kawai, S. Sato, K.J. Ishii, C. Coban, H. Hemmi, M. Yamamoto, K. Terai, M. Matsuda, J. Inoue, S. Uematsu, O. Takeuchi, S. Akira, Interferon-[alpha] induction through Toll-like receptors involves a direct interaction of IRF7 with MyD88 and TRAF6, Nat. Immunol. 5 (2004) 1061–1068.
[23] K. Honda, Y. Ohba, H. Yanai, H. Negishi, T. Mizutani, A. Takaoka, C. Taya, T. Taniguchi, Spatiotemporal regulation of MyD88-IRF-7 signalling for robust type-I interferon induction, Nature 434 (2005) 1035–1040.
[24] J.C. Kagan, R. Medzhitov, Phosphoinositide-mediated adaptor recruitment controls Toll-like receptor signaling, Cell 125 (2006) 943–955.
[25] T. Nishiya, E. Kajita, T. Horinouchi, A. Nishimoto, S. Miwa, Distinct roles of TIR and non-TIR regions in the subcellular localization and signaling properties of MyD88, FEBS Lett. 581 (2007) 3223–3229.
[26] K. Burns, F. Martinon, C. Esslinger, H. Pahl, P. Schneider, J.-L. Bodmer, F. Di Marco, L. French, J. Tschopp, MyD88, an adapter protein involved in interleukin-1 signaling, J. Biol. Chem. 273 (1998) 12203–12209.
[27] H. Hacker, V. Redecke, B. Blagoev, I. Kratchmarova, L.-C. Hsu, G.G. Wang, M.P. Kamps, E. Raz, H. Wagner, G. Hacker, M. Mann, M. Karin, Specificity in Toll-like receptor signalling through distinct effector functions of TRAF3 and TRAF6, Nature 439 (2006) 204–207.
[28] Z. Jiang, P. Georgel, C. Li, J. Choe, K. Crozat, S. Rutschmann, X. Du, T. Bigby, S. Mudd, S. Sovath, I.A. Wilson, A. Olson, B. Beutler, Details of Toll-like receptor:adapter interaction revealed by germ-line mutagenesis, Proc. Natl. Acad. Sci. USA 103 (2006) 10961–10966.
[29] H.H. Park, E. Logette, S. Raunser, S. Cuenin, T. Walz, J. Tschopp, H. Wu, Death domain assembly mechanism revealed by crystal structure of the oligomeric PIDDosome core complex, Cell 128 (2007) 533–546.
[30] M.C. Moncrieffe, J.G. Grossmann, N.J. Gay, Assembly of oligomeric death domain complexes during toll receptor signalling, J. Biol. Chem. 283 (2008) 33447–33454.